Time-Frequency Packing for Linear Modulations: Spectral Efficiency and Practical Detection Schemes

Alan Barbieri, Dario Fertonani, *Student Member, IEEE*, and Giulio Colavolpe, *Member, IEEE*

***Abstract*—We investigate the spectral efficiency, achievable by a low-complexity symbol-by-symbol receiver, when linear modulations based on the superposition of uniformly time- and frequency-shifted replicas of a base pulse are employed. Although orthogonal signaling with Gaussian inputs achieves capacity on the additive white Gaussian noise channel, we show that, when finite-order constellations are employed, by giving up the orthogonality condition (thus accepting interference among adjacent signals) we can considerably improve the performance, even when a symbol-by-symbol receiver is used. We also optimize the spacing between adjacent signals to maximize the achievable spectral efficiency. Moreover, we propose a more involved transmission scheme, consisting of the superposition of two independent signals with suitable power allocation and a two-stage receiver, showing that it allows a further increase of the spectral efficiency. Finally, we show that a more involved equalization algorithm, based on soft interference cancellation, allows to achieve an excellent bit-error-rate performance, even when error-correcting codes designed for the Gaussian-noise-limited channel are employed, and thus does not require a complete redesign of the coding scheme.**

***Index Terms*—Linear modulations, interchannel interference, multiuser channels, information rate, spectral efficiency.**

I. Introduction

We consider linear modulations over an additive white Gaussian noise (AWGN) channel. The transmitted signal is the superposition of time- and frequency-shifted replicas of a base pulse multiplied by channel symbols belonging to a complex constellation. As common in the literature (e.g., see [1]–[3]) a uniform rectangular tiling of the time-frequency domain is considered. Hence, the signal model is completely defined by the base pulse and the distance between adjacent symbols in the time and frequency domains, denoted by T and F, respectively. Note that, with respect to [1]–[3], we consider flat channels only, although all ideas underlying this paper could be extended to frequency-selective channels as well. It is clear that T and F play an important role, since on one hand they establish the efficiency in the usage of the available time and frequency resources, and at the same time their values determine the amount of interference (if present) a signal brings to the adjacent ones.

Paper approved by H. Leib, the Editor for Communication and Information Theory of the IEEE Communications Society. Manuscript received April 18, 2008; revised October 24, 2008.

A. Barbieri and D. Fertonani are with the Scuola Superiore Sant'Anna, 56124 Pisa, Italy (e-mail: a.barbieri@sssup.it, dario.fertonani@gmail.com).

G. Colavolpe is with the Department of Information Engineering, University of Parma, 43100 Parma, Italy (e-mail: giulio@unipr.it).

This work has been presented in part at the IEEE International Symposium on Information Theory (ISIT '08), Toronto, Canada, July 2008.

Digital Object Identifier 10.1109/TCOMM.2009.10.080200

A common choice in the literature is the use of orthogonal signaling, that ensures absence of interference. Rectangular or sinc pulses with orthogonal signaling are employed in orthogonal frequency division multiplexing (OFDM), which is known to be optimal from an information theoretic point of view when independent Gaussian distributed input symbols are used. Hence, constellations and practical coding schemes are often designed such as to ensure an approximately Gaussian input [4]. On the contrary, it is known that, when finite-order constellations are considered (e.g., phase shift keying (PSK) or quadrature amplitude modulation (QAM)), the efficiency of the communication system can be improved by giving up the orthogonality condition. For example, faster-than-Nyquist signaling [6], [7] is a well known technique consisting of reducing the spacing in the time-domain well below the Nyquist rate, thus introducing controlled inter-symbol interference (ISI). In [8] the joint optimization of both time and frequency spacing is considered, by finding their smallest values that ensure no reduction of the minimum Euclidean distance, with respect to the Nyquist case. In order for those techniques to be effective, a receiver able to cope with the (possibly very large) interference, stemming from the lack of orthogonality, is assumed. The computational complexity of such a receiver may be extremely large, and no hints are given by those paper regarding the optimization in the more practical scenario where a trivial symbol-by-symbol receiver is employed.

Although our goal in this paper is similar to the above mentioned works, we pursue here a different approach for the optimization of the spacing values T and F. We fix the base pulse[1] and we evaluate the information rate, achievable by a symbol-by-symbol receiver, as a function of the spacing values. Eventually, we optimize the spacings such as to maximize the achievable spectral efficiency of the communication system. The considered problem is relevant since it turns out that improving the spectral efficiency without increasing the constellation order, e.g., by using a quaternary PSK (QPSK), can be considerably convenient, since the decoding complexity increases as the constellation size increases. Moreover, it is well known that low-order constellations are more robust to channel impairments such as time-varying fading or phase noise [5].

Furthermore, we propose a more involved transmission scheme, consisting of the superposition of two independent signals belonging to rectangular time-frequency lattices (being

[1]We consider pulses commonly employed in practical systems, namely rectangular (REC), Gaussian, and pulses whose spectrum is root raised cosine (RRC) shaped—for simplicity the latter will be denoted as RRC pulses.

the two lattices properly staggered), with a suitable power allocation between the two signals, and a two-stage receiver that proceeds as follows: symbol-by-symbol detection of the first set of signals is carried out, followed by decoding, and the corresponding hard-decisions are used to mitigate the interference caused by the first set to the second one. Finally, symbol-by-symbol detection of the second set of signals is carried out based on the interference-mitigated received samples. We show that the spectral efficiency achievable by the proposed scheme is considerably high, even when a low-order constellation, such as QPSK, is used. Finally, although all the information-theoretic results will be obtained assuming a symbol-by-symbol receiver, the bit-error-rate (BER) performance of a suitably designed receiver based on soft interference cancellation (SIC) [9], [10] will be assessed as well. We will show that such a receiver exhibits an excellent BER performance despite the presence of strong interference, even when error-correcting codes designed for the AWGN channel are employed, thus without the need for a complete redesign of the coding scheme.

The novelty of the ideas and methods proposed in this paper can be summarized in three aspects: first, we consider the *spectral efficiency* as our performance measure, rather than the minimum distance. Second, we consider a low-complexity *symbol-by-symbol* detection algorithm at the receiver, characterized by a negligible complexity *irrespectively of the interference set size*, rather than more complex algorithms such as the Viterbi or linear equalizers employed in [6]–[8]. This makes our approach more realistic, since those algorithms may be unfeasible in strongly interfered channels, i.e., when the optimal values of T and/or F are small. We point out that, with our approach, also the *optimization* of the spacing values takes into account the presence of a symbol-by-symbol receiver. Third, we propose a transmission scheme based on the superposition of two independent signals with a suitable staggering and power allocation, showing that the achievable spectral efficiency can be dramatically increased, with only a negligible increase in the computational complexity of the receiver.

The remainder of this paper is organized as follows. In Section II, we give the system model, while in Section III we address the related ultimate performance limits. In Section IV we describe an algorithm for optimizing the achievable spectral efficiency, while in Section V a novel transmission scheme based on the superposition of two independent signals is proposed. In Section VI a practical equalization algorithm for the considered problem, based on the SIC framework, is described. Finally, in Section VII, the effectiveness of the spectral efficiency optimization algorithm is proved by numerical simulation results. Moreover, in the same section a convergence threshold analysis based on extrinsic information transfer (EXIT) charts [11], and the corresponding BER performance, are assessed for a practical low-density parity check (LDPC) [12] coded system. Finally, Section VIII gives some concluding remarks.

II. System Model

We consider a linear modulation, where the base pulse $p(t)$ is regularly shifted in the time and frequency domains, of multiples of T seconds and F Hz respectively. We assume a perfect synchronization among the data streams (downlink assumption) and that the transmitted symbols $\{x_{n,k}\}$ (being n the time index and k the carrier index) belong to a given zero-mean M-th order complex constellation and are independent and uniformly distributed (i.u.d.), i.e.,

$$\begin{aligned} \mathbb{E}\{x_{n,k}\} &= 0 \\ \mathbb{E}\{x_{n,k}x^*_{n',k'}\} &= \delta(n-n')\delta(k-k') \end{aligned} \tag{1}$$

where $\delta(\cdot)$ denotes the Kronecker delta. Under the above assumptions, the baseband transmitted signal reads [1], [2][2]

$$x(t) = \sqrt{E_S TF}\sum_n \sum_k x_{n,k} p(t-nT)e^{j2\pi kFt} \tag{2}$$

where the factor $\sqrt{TF}$ has the important aim of normalizing the signal power, such as to ensure a constant average power spectral density (PSD), irrespectively of T and F [1]. We point out that this normalization is arbitrary, and a different choice would have been acceptable as well. For example, when a frequency division multiplexed (FDM) multi-user scenario is considered, namely when the index k in (2) denotes signals coming from different users, a reasonable choice is to normalize the average power of each user, rather than the average PSD. Hence, with this choice the normalization factor in front of (2) would become $\sqrt{E_S}$ instead of $\sqrt{E_S TF}$. This would lead to slightly different simulation results with respect to those obtained in this paper, although the general conclusions still remain unchanged. Note that the summations in (2) extend from $-\infty$ to $+\infty$, namely an infinite number of time epochs and of carriers are employed [1]. The base pulse $p(t)$ can be an RRC pulse with roll-off factor α, an REC pulse, or a Gaussian pulse. Gaussian pulses will be analyzed thanks to their time-frequency compactness property [13]. Without loss of generality, we will normalize the employed pulses in the time domain such that the RRC pulse has bandwidth $1+\alpha$, the REC pulse has a duration of 1, and the Gaussian pulse has the same standard deviation in both time and frequency domains (symmetry assumption) [1]. Moreover, the base pulse will be assumed of unitary energy.

At the receiver, we assume that a filter matched to the time-frequency shifted replicas of the base pulse is employed, together with a symbol-by-symbol detection algorithm [2]. Note that this is the optimal choice in the maximum a posteriori (MAP) sense, only if the signals

$$\{p(t-nT)e^{j2\pi kFt}\}_{n,k} \tag{3}$$

are mutually orthogonal. On the contrary, when orthogonality is not ensured, interference among the signals arises and the MAP criterion leads to a more involved receiver, whose complexity depends exponentially on the cardinality of the interference set. The set of signals in (3) is denoted as a *Weil-Heisenberg* system of functions [1]. As it will be clear from the next sections, the product TF (i.e., the lattice size of the

[2]We point out that more general signal structures were proposed in the literature, for example based on hexagonal lattices [2]. Although we investigated those signaling schemes also, the relevant results are not reported here since the improvements they provide in terms of spectral efficiency are negligible.

time-frequency grid) is of paramount importance in defining the performance of the considered communication system.

Since we assumed in (2) an infinite amount of signals, without loss of generality in the rest of this paper we will consider the problem of detecting the signal $x_{0,0}$ only. Since symbol-by-symbol detection is considered, the only observed sample employed in the detection reads

$$y_{0,0} = \int y(t)p^*(t)dt = \int [x(t) + w(t)]p^*(t)dt \qquad (4)$$

where an AWGN channel is considered, $w(t)$ being a circularly symmetric zero-mean white Gaussian process with PSD equal to N_0. By joining (2) and (4), we eventually obtain

$$y_{0,0} = \sqrt{E_S TF}\sum_n \sum_k x_{n,k}A_p(nT, kF) + z_{0,0} \qquad (5)$$

where $A_p(\tau, \nu)$ is the *ambiguity function* [2], defined as[3]

$$A_p(\tau, \nu) = \int p(t-\tau)p^*(t)e^{j2\pi\nu t}dt \qquad (6)$$

that depends only on the base pulse $p(t)$ (e.g., if $p(t)$ is Gaussian, then $A_p(\tau, \nu)$ is bi-variate Gaussian). The additive noise term $z_{0,0}$ is $z_{0,0} = \int w(t)p^*(t)dt$. We remark that $z_{n,k}$ is colored unless the signals (3) are orthogonal. However, the performance of a receiver which carries out symbol-by-symbol detection depends only on the variance of $z_{0,0}$, given by N_0.

Note that (5) can be rewritten as

$$y_{0,0} = \sqrt{E_S TF}x_{0,0} + \sqrt{E_S TF}\sum_{(n,k)\neq(0,0)} x_{n,k}A_p(nT, kF) + z_{0,0} \qquad (7)$$

where the two different impairments experienced by the receiver, namely the background noise and the interference due to adjacent signals, are pointed out [14]. The Gaussian pulse has the highest energy compactness jointly in time and frequency [13], and is therefore widely considered in the literature [1], [2].

Instead of simply neglecting the interference due to adjacent signals in (7), we pursue here a more general approach, which consists of modeling the interference as a zero-mean Gaussian process with PSD equal to N_I, of course independent of the additive thermal noise—we point out that this approximation is exploited only by the receiver, while in the actual channel the interference is clearly generated as in (7). Note that the interference is really Gaussian distributed only if the transmitted symbols $x_{n,k}$ are Gaussian distributed as well. Approximating the interference as Gaussian even when the constellation is finite, is common in the multi-user literature (see, e.g., [15]). We remark that, especially when the interference set is small, e.g., when T and F are large, actual interference distribution may substantially differ from a Gaussian distribution. However, we point out that the accuracy of this approximation is not of concern here: assuming Gaussian-distributed interference is anyway required to ensure that a symbol-by-symbol receiver is optimal, according to the MAP criterion, for the assumed channel model. Namely, it is like to say that the Gaussian assumption is a *consequence* of the choice of the symbol-by-symbol receiver.

With the above mentioned Gaussian approximation, the channel model assumed by the receiver is

$$y_{n,k} = \sqrt{E_S TF}x_{n,k} + v_{n,k} \qquad (8)$$

where $\{v_{n,k}\}$ are independent and identically distributed zero-mean circularly symmetric Gaussian random variables, with variance $N_0 + N_I$. It turns out that

$$N_I = E_S TF \sum_{(n,k)\neq(0,0)} |A_p(nT, kF)|^2 \qquad (9)$$

where the independence of the transmitted symbols has been used.

III. Ultimate Performance Limits

We are interested in evaluating the ultimate performance limits achievable by a symbol-by-symbol receiver designed for the auxiliary channel (8) when the actual channel is that in (7), in terms of information rate and spectral efficiency. This issue is an instance of *mismatched* decoding [16] (see also [17]). The achievable information rate (AIR), measured in bit per channel use, for the mismatched receiver yields

$$I(x_{0,0}; y_{0,0}) = E_{x_{0,0}, y_{0,0}}\left\{\log_2 \frac{M p_{Y_{0,0}|X_{0,0}}(y_{0,0}|x_{0,0})}{\sum_x p_{Y_{0,0}|X_{0,0}}(y_{0,0}|x)}\right\} \qquad (10)$$

where $p_{Y_{0,0}|X_{0,0}}(y_{0,0}|x_{0,0})$ is a Gaussian probability density function (pdf) of mean $\sqrt{E_S TF}x_{0,0}$ and variance $N_0 + N_I$ (in accordance with the auxiliary channel model (8)), while the outer statistical average, with respect to $x_{0,0}$ and $y_{0,0}$, is carried out according to the real channel model (7) [14], [17]. Eq. (10) can be evaluated efficiently by means of a Monte Carlo average. Let us recall that the mismatched receiver can assure error-free transmissions when the provided information rate does not exceed $I(x_{0,0}; y_{0,0})$ in (10).

From a system viewpoint, the spectral efficiency, that is the amount of information transmitted per unity of time and per unity of bandwidth, is a more significant quality figure than the information rate. Hence, the derivation of the spectral efficiency for the considered system is given in the following. First, we notice that the *overall* information rate (in bits per channel use) achievable by the symbol-by-symbol receiver when $2N+1$ time epochs and $2K+1$ carriers are employed, is given by

$$\sum_{n=-N}^{N}\sum_{k=-K}^{K} I(x_{n,k}; y_{n,k})$$

while the signal duration and bandwidth are proportional to $2N+1$ and $2K+1$, respectively, plus some additive terms independent of N and K and taking into account the pulse tails in time and frequency. Thus, for increasingly large values of N and K the boundary effects become negligible for the *overall* information rate, the *overall* duration, and the *overall* bandwidth. Hence, under the assumption of infinite transmission in both the time and the frequency domain, the achievable spectral efficiency (ASE) yields

$$\eta = \frac{1}{FT} I(x_{0,0}; y_{0,0}) \quad \left[\frac{\text{bit}}{\text{s}\cdot\text{Hz}}\right]. \qquad (11)$$

[3]We point out that (6) differs from the definition employed in [2] for an unimportant multiplicative factor of unitary magnitude.

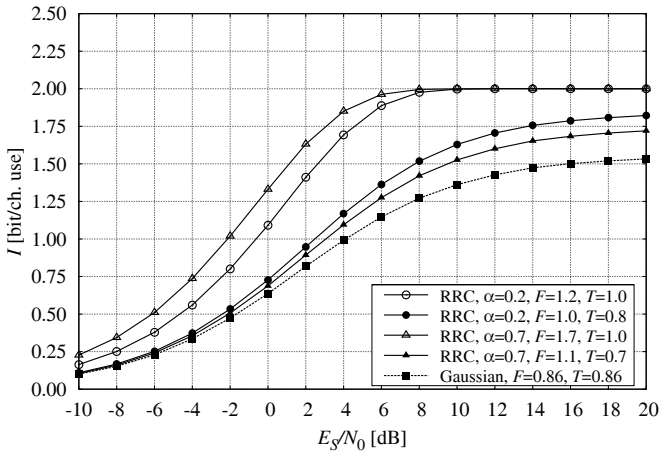

Fig. 1. AIR of a QPSK modulation for several pulses and values of the spacing.

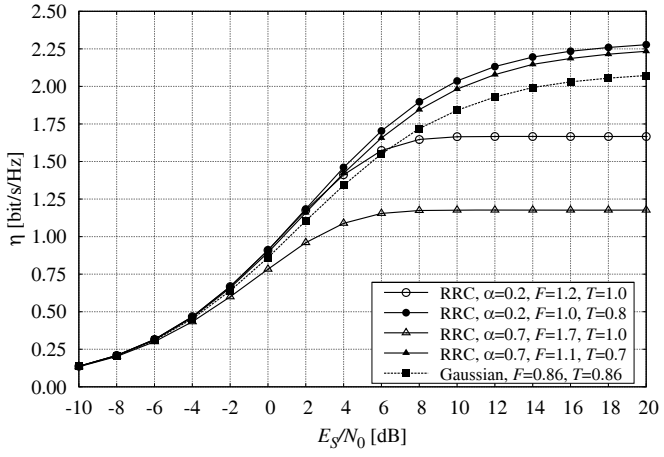

Fig. 2. ASE of a QPSK modulation for several pulses and values of the spacing.

As a consequence, thanks to the assumption of a large number of signals in both time and frequency domains, we can keep focusing on the information stream $x_{0,0}$ even for evaluating the ASE.

Some simulation results are reported in Fig. 1, which shows how the AIR varies with the value of E_S/N_0 when different values of the time and frequency spacings T and F are considered, for RRC and Gaussian pulses and QPSK symbols. Note that, for the RRC pulse with roll-off factor α, when $T = 1$ and $F \geq 1 + \alpha$ the resulting signals (3) are mutually orthogonal, thus $A_p(nT, kF) = 0$ for each $(n, k) \neq (0, 0)$ and the interference term disappears from (7). In this case, $N_I = 0$ and the auxiliary channel (8) becomes equivalent to the real channel (7). The two curves with $T = 1$ and $F = 1 + \alpha$ in Fig. 1 can therefore be interpreted as interference-free benchmark curves.

We point out that the difference, in terms of AIR, between the two considered orthogonal signaling formats stems from the normalization factor $\sqrt{FT}$ introduced in (2). Fig. 1 gives a quantitative evidence of the fact that the lower the values of T or F, the larger the interference due to the adjacent signals, and therefore the smaller the resulting AIR. We remark again that the values of information rate shown in Fig. 1 are *achievable* by a MAP symbol-by-symbol receiver designed for the channel model (8).

On the other hand, very interesting insights are given by the results reported in Fig. 2, which shows the ASE corresponding to the same modulation formats as in Fig. 1. These results clarify that the values of T and F providing the best AIR are not those providing the best ASE, and thus that a careful design strategy, when the spectral efficiency is the key quality figure, should trade an intentional degradation in AIR for a larger ASE.

For instance, in the case of the RRC pulse with roll-off factor $\alpha = 0.7$, the choice $T = 0.7$ and $F = 1.1$ provides a spectral efficiency significantly larger than the choice $T = 1.0$, $F = 1.7$, namely the minimum spacing that ensures orthogonality. Moreover, despite the ambiguity function $A_p(\tau, \nu)$ of the Gaussian pulse is strictly larger than 0 for each τ and ν (thus interference is always present, irrespectively of the values of T and F), the Gaussian pulse outperforms, in terms of achievable spectral efficiency, the orthogonal signal sets based on RRC pulses, at least for vanishing small noise power.

IV. Optimization of the Spectral Efficiency

Our aim is to find, for a given constellation and base pulse, the spacings T and F that provide the largest ASE. In general, we could expect that the optimal spacings depend on the signal-to-noise ratio (SNR). To this purpose, we plotted (not shown here for a lack of space) the ASE as a function of T and F and for different values of E_S/N_0. As the SNR increases, not only the ASE increases, but also the optimal values of the spacing change. For $E_S/N_0 \to \infty$, the maximal ASE for the RRC pulse with $\alpha = 0.2$ is achieved with $T = 0.8$ and $F = 1.0$, i.e., the values previously employed in Fig. 1. However, since we noticed that the dependence of the optimal spacing values on the SNR is usually very limited, and in order to simplify computer simulations, we decided to carry out the optimization only asymptotically, i.e., for vanishing small noise power, and evaluate the ASE at any SNR using the spacings that are asymptotically optimal.

The properties of the function $\eta(T, F)$ cannot be easily studied in closed form,[4] but it reads clear, by physical arguments, that it is bounded, continuous in T and F, and tends to zero when $T, F \to 0$ or $T, F \to \infty$. Hence, the function $\eta(T, F)$ has a maximum value—according to our findings, in most cases there are no local maxima other than the global maximum. Formally, for a given modulation format, base pulse, and value of E_S/N_0, the optimization problem consists of finding the maximal ASE

$$\eta_{\mathsf{M}}(E_S/N_0) = \max_{T>0, F>0} \eta(T, F, E_S/N_0) \tag{12}$$

which can be solved by evaluating $\eta(T, F, E_S/N_0)$ on a grid of values of T and F (coarse search), followed by an interpolation of the obtained values (fine search).

[4]Although the functions AIR $I(\cdot)$ and ASE $\eta(\cdot)$ depend on various system parameters, in the following we will only explicitly indicate the parameters of interest for the relevant discussion.

V. Double Signaling with Interference Cancellation

So far, a significant increase in the ASE was achieved by intentionally introducing controlled interference among adjacent signals, in order to make a better use of the available resources (time and frequency). Inspired by the same rationale, we propose a more involved way to improve the ASE, with only a minor increase of the computational complexity at the receiver. The idea is to combine two independent signals, each of them belonging to a rectangular time-frequency lattice (being the two lattices properly staggered), with a suitable power allocation between the two signals. The transmitted signal reads[5]

$$x(t) = \sqrt{(1-\beta^2)E_S FT}\sum_{n,k}\dot{x}_{n,k}p(t-nT)e^{j2\pi kFt} + \beta\sqrt{E_S FT}\sum_{n,k}\ddot{x}_{n,k}p(t-(n+1/2)T)e^{j2\pi(k+1/2)Ft} \tag{13}$$

where $\beta \in [0,1]$ is the power allocation factor, $\{\dot{x}_{n,k}\}$ and $\{\ddot{x}_{n,k}\}$ both satisfy (1), and $\mathbb{E}\{\dot{x}_{n,k}\ddot{x}^*_{n',k'}\} = 0$ for each n, n', k, k'. The constant multiplicative factors in (13) ensure a constant average PSD independently on T, F, and β. The sequences $\{\dot{x}_{n,k}\}$ and $\{\ddot{x}_{n,k}\}$ are the output of two separate encoders, with rate $\dot{R}$ and $\ddot{R}$, respectively. Note that, for $\beta = 0$ or $\beta = 1$, a signal equivalent to (2) results.

At the receiver, whose frontend is again composed by a bank of matched filters, the following operations are carried out. First, the samples

$$\dot{y}_{n,k} = \int y(t)p^*(t-nT)e^{-j2\pi kFt}dt$$

($y(t)$ being the continuous-time received signal) are employed to perform a symbol-by-symbol detection of the transmitted symbols $\dot{x}_{n,k}$. It is worth noting that, besides the self-interference as described in (7), samples $\dot{y}_{n,k}$ are affected by the interference due to the secondary symbols $\ddot{x}_{n,k}$ as well, thus the parameter N_I of the auxiliary channel model (8) must take into account the increased interference power. Therefore, we expect that the AIR $I(\dot{x}_{0,0};\dot{y}_{0,0})$, which of course depends on the SNR, the base pulse, and the spacings T and F, rapidly decreases for increasingly large values of β. However, assuming that $0 < \dot{R} < I(\dot{x}_{0,0};\dot{y}_{0,0})$, there exists a rate-$\dot{R}$ code that ensures an arbitrarily small probability of error for the hard decisions of the symbols $\dot{x}_{n,k}$. Consequently, after successful decoding of the symbols $\dot{x}_{n,k}$ has been carried out, the following interference-mitigation operation is performed

$$\ddot{y}(t) = y(t) - \sqrt{(1-\beta^2)E_S FT}\sum_{n,k}\dot{x}_{n,k}p(t-nT)e^{j2\pi kFt} \tag{14}$$

and the samples

$$\ddot{y}_{n,k} = \int \ddot{y}(t)p^*(t-(n+1/2)T)e^{-j2\pi(k+1/2)Ft}dt$$

are employed to perform symbol-by-symbol detection of the secondary sequence $\{\ddot{x}_{n,k}\}$. In order to ensure arbitrarily small probability of error for the detection of the secondary sequence as well, it must be $0 < \ddot{R} < I(\ddot{x}_{0,0};\ddot{y}_{0,0})$.

The overall AIR of the proposed method is the sum of the AIRs of the two sequences, and the ASE is the ratio between the overall AIR and FT. We remark that the power allocation parameter β plays a key role, and must be optimized in order to maximize the overall AIR. We denote by β_{OPT} the optimized parameter. For vanishing small noise power, the following proposition holds.

Proposition: If $E_S/N_0 \to \infty$, $AIR(\beta)$ is continuous on $(0,1]$ (rather than on the closed interval $[0,1]$), it is strictly decreasing in $(0,1]$, and $AIR(\beta = 0) = AIR(\beta = 1)$. Its supremum

$$\sup_{\beta} AIR(\beta) = \lim_{\beta\to 0^+} AIR(\beta) \tag{15}$$

is doubled with respect to the case of a single signal (10), when the base pulse and the spacing values T and F are fixed. Moreover, the supremum is not attained by any value of $\beta \in [0,1]$.

Note that, when the SNR is bounded, the factor of increase of the AIR is strictly less than 2, and β_{OPT} must be optimized numerically.

Proof: First of all, note that $AIR = \dot{R}+\ddot{R}$. In the absence of thermal noise, from the definition of achievable information rate, it turns out that $\dot{R}$ is a continuous function of β, since the expectation is a linear operator and the integrand function is a continuous function of β, for $\beta \in [0,1]$. Moreover, $\dot{R}$ is decreasing in β, since β determines the signal-to-interference ratio. On the other hand, since due to (14) the samples $\ddot{y}_{n,k}$ are not affected by the interference due to the first signal, and since the signal-to-noise ratio is infinite irrespectively of β (as long as $\beta > 0$), $\ddot{R}$ is constant for $\beta \in (0,1]$ and is null for $\beta = 0$. This proves the claims regarding monotonicity and continuity. Moreover, from the monotonicity of $\dot{R}$ and the step shape of $\ddot{R}$, (15) is immediately proved. Finally, note that the same signaling scheme is obtained for $\beta = 0$ and $\beta = 1$ (with only an exchange between the two signals), thus the corresponding AIRs are the same. ◇

In Fig. 3, the spectral efficiency achievable by the proposed receiver based on interference mitigation, when the transmitted signal is (13), is shown as a function of the power allocation factor β. A QPSK modulation and an RRC pulse with $\alpha = 0.2$, $T = 0.8$, $F = 1.0$, and several values of E_S/N_0 have been used. As it can be seen, for very small values of the SNR, the ASE is almost independent of β, and basically no improvements are obtained when a signal format as in (13) is employed (i.e., when $\beta > 0$). On the contrary, for increasingly large values of the SNR, the gain provided by the proposed scheme becomes larger and larger, whereas β_{OPT} rapidly decreases to 0.

VI. Low-Complexity Equalization

Although a symbol-by-symbol receiver has been assumed throughout this paper, in particular circumstances the interference among adjacent symbols could be strong enough to require a suitable design of the coding scheme, since in these

[5]We point out that the transmitted signal in (13) falls under the general model of multi-pulse multi-carrier (MPMC) modulations of [3]. However, we remark that, as opposed to [3], we do not look for orthogonal pulses, we (partially) deal with interference at the receiver, and we employ finite-order constellations.

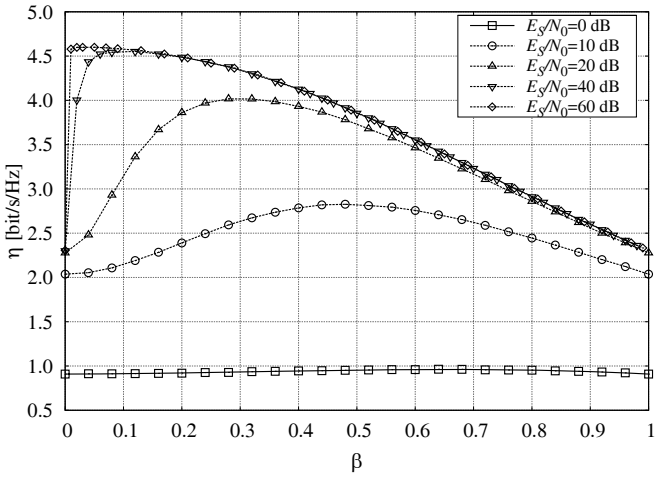

Fig. 3. ASE of the proposed interference-mitigation receiver and double signaling, as a function of the power allocation factor β, for a QPSK modulation and an RRC pulse with $\alpha = 0.2$, $T = 0.8$, and $F = 1.0$.

cases error-correcting codes designed for the interference-free AWGN channel fail to achieve reliable communication at the SNR values predicted by the information-theoretic analysis. An effective way to avoid such a complete redesign of the coding scheme is the use of a more involved equalization algorithm at the receiver, as that proposed in this section, based on the well known soft interference cancellation principle and inspired by the wide literature on multiuser detection (see, e.g., [9], [10] and references therein). The resulting algorithm may be employed as a soft-input soft-output (SISO) block in iteratively decoded concatenated "turbo" schemes, according to the turbo-equalization principle [18]. However, we remark that it is not possible to evaluate the information rate, achievable by the proposed SIC-based receiver, using the tools described in Section III, since there does not exist an auxiliary channel for which the proposed SIC receiver is an instance of the exact MAP criterion. Therefore, the performance of the proposed equalization algorithm will be assessed, in Section VII, in terms of convergence threshold and BER only.

Assume that, at a given iteration, the equalization algorithm is activated with a set of a priori probabilities, coming from the SISO decoder, equal to $\{P(x_{n,k})\}$ (in such concatenated schemes, the code symbols are usually assumed independent). The algorithm proceeds as follows:

1) $iter = 0$ and the extrinsic probabilities $p^{(iter)}(\mathbf{y}|x_{n,k})$ are initialized to a constant value (we denote with $\mathbf{y}$ the set of all the observed samples belonging to the current codeword);
2) the a posteriori mean and variance of every code symbol is evaluated according to

$$\mu_{n,k} = \sum_{\ell=0}^{M-1} x^{(\ell)} P(x_{n,k} = x^{(\ell)}|\mathbf{y}) \tag{16}$$

$$\simeq \sum_{\ell=0}^{M-1} x^{(\ell)} P(x_{n,k} = x^{(\ell)}) \frac{p^{(iter)}(\mathbf{y}|x_{n,k} = x^{(\ell)})}{p^{(iter)}(\mathbf{y})}$$

$$\sigma^2_{n,k} = \sum_{\ell=0}^{M-1} |x^{(\ell)}|^2 P(x_{n,k} = x^{(\ell)}|\mathbf{y}) - |\mu_{n,k}|^2 \tag{17}$$

$$\simeq \sum_{\ell=0}^{M-1} |x^{(\ell)}|^2 P(x_{n,k} = x^{(\ell)}) \frac{p^{(iter)}(\mathbf{y}|x_{n,k} = x^{(\ell)})}{p^{(iter)}(\mathbf{y})} - |\mu_{n,k}|^2$$

where the complex values $x^{(\ell)}$, $\ell = 0, \ldots, M-1$, denote all the constellation symbols of the M-ary alphabet. Note that, in (16) and (17), $p^{(iter)}(\mathbf{y})$ plays the role of a constant normalization factor, and in fact need not to be evaluated or stored;

3) the interference is removed from all the received samples according to

$$\tilde{y}_{n,k} = y_{n,k} - \sqrt{E_S TF} \sum_{(m,i)\in\mathcal{I}} A_p(mT, iF)\mu_{n+m,k+i}$$

where $\mathcal{I}$ denotes the interference set. Although in general $\mathcal{I} = \{(m,i) : |m| + |i| \neq 0\}$, in practice only the symbols adjacent to the considered one contribute to interference, since $A_p(mT, iF)$ rapidly decreases when $|m|$ or $|i|$ become large. Therefore, we will use $\mathcal{I} = \{(m,i) : |m| \leq L_T, |i| \leq L_F, |m|+|i| \neq 0\}$, being L_T and L_F design parameters;
4) a symbol-by-symbol evaluation of the extrinsic probabilities is carried out by assuming independent and Gaussian distributed $\{\tilde{y}_{n,k}\}$, namely

$$p^{(iter+1)}(\mathbf{y}|x_{n,k}) \propto \exp\left[-\frac{|\tilde{y}_{n,k} - \sqrt{E_S TF} x_{n,k}|^2}{\Sigma_{n,k}}\right]$$

where

$$\Sigma_{n,k} = N_0 + E_S TF \sum_{(m,i)\in\mathcal{I}} |A_p(mT, iF)|^2 \sigma^2_{n+m,k+i}\,;$$

5) $iter = iter + 1$; if $iter < SI$ (the design parameter SI being the overall number of self-iterations) return to 2, otherwise continue;
6) the extrinsic probabilities fed to the SISO decoder are $\{p^{(SI)}(\mathbf{y}|x_{n,k})\}$.

We remark that the computational complexity of the proposed SIC algorithm is in general very limited, and only slightly larger than that of the plain symbol-by-symbol detector. In particular, the complexity depends linearly on the codeword size, the number of self-iterations, the constellation size, and the cardinality of the interference set $\mathcal{I}$. Moreover, we point out that the proposed algorithm does not involve any sequential operation, and can thus be implemented fully parallel, with a latency of the same order of magnitude of the symbol-by-symbol receiver. The performance of the proposed receiver in practical scenarios will be assessed in Section VII.

We also point out that, when the proposed SIC-based receiver is employed as the SISO turbo-equalization block in iteratively decoded schemes, some of the self-iterations can be saved by introducing memory between consecutive iterations of the overall detection and decoding scheme. In particular, a smart solution that allows excellent performance, as we will show in Section VII, with limited computational complexity, consists in avoiding the reset of messages $p^{(0)}(\mathbf{y}|x_{n,k})$ carried out at step 1), that instead can be initialized with the extrinsic probabilities evaluated in the previous run of the equalization block. In this way, even if only one self-iteration is carried out, the performance in an iteratively-decoded scheme may

TABLE I
ASYMPTOTIC (I.E., FOR VANISHING SMALL NOISE POWER) ASE.

Constell.	Pulse	Sig. mod.	T_{opt}	F_{opt}	Orthog.	η
QPSK	REC	eq. (2)	1.00	1.00	Yes	2.00
QPSK	REC	eq. (2)	1.00	0.80	No	2.32
QPSK	RRC-0.2	eq. (2)	1.00	1.20	Yes	1.67
QPSK	RRC-0.2	eq. (2)	0.80	1.00	No	2.28
QPSK	RRC-0.7	eq. (2)	1.00	1.70	Yes	1.18
QPSK	RRC-0.7	eq. (2)	0.72	1.10	No	2.27
16-QAM	RRC-0.2	eq. (2)	1.00	1.20	Yes	3.33
16-QAM	RRC-0.2	eq. (2)	0.95	1.05	No	3.95
QPSK	Gauss.	eq. (2)	0.88	0.88	No	2.10
QPSK	Gauss.	eq. (13)	0.88	0.88	No	4.21
16-QAM	Gauss.	eq. (2)	1.15	1.15	No	5.43

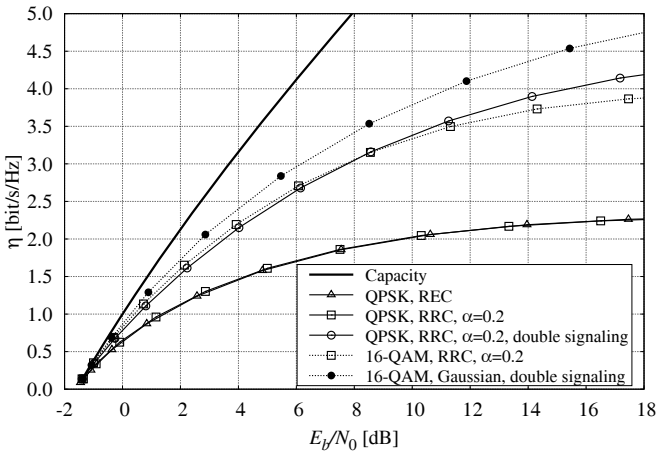

Fig. 4. ASE, as a function of E_b/N_0, for a set of selected cases.

in practice approach that of the algorithm carrying out many self-iterations. The resulting algorithm will be denoted as no-message-resetting (NMR) SIC algorithm.

VII. NUMERICAL RESULTS

In this section, the maximal ASE, obtained with a proper optimization of the spacing parameters T and F (and β when double signaling is considered), is evaluated for several modulation formats and base pulses. For comparison purposes, the capacity per unity of bandwidth $\eta_C = \log_2(1 + E_S/N_0)$ of the considered AWGN channel in terms of bit/s/Hz, is also shown. Note that the above spectral efficiency is achieved by Gaussian-distributed input symbols and orthogonal signaling.

Table I collects the performance, in terms of asymptotic (i.e., for vanishing small thermal noise power) maximal ASE, of a set of modulation formats and base pulses. For all the considered formats based on REC and RRC pulses, the performance for orthogonal signaling (i.e., when $T = 1$ and $F = 1 + \alpha$ for RRC and $T = F = 1$ for REC) is shown for comparison. This Table summarizes the significant gain in terms of ASE provided by the techniques proposed in this paper. Note that the asymptotic spectral efficiency, achievable by modulations based on REC pulse or RRC pulses with completely different values of the roll-off factor, is almost the same when optimization of the spacing values is carried out. This stems from the fact that pulses with a larger roll-off can be squeezed more in the time-domain, and viceversa. The product of the optimal T and F is almost the same in the considered scenarios, as well as the asymptotic AIR. Moreover, we point out that the larger the constellation size, the smaller the performance gain achieved with a suitable optimization of the spacing values. An important fact, confirmed by these simulation results, is that the loss in terms of ASE of orthogonal signaling with respect to the optimized case rapidly decreases as the constellation size increases (we remark again that, when the input symbols are i.u.d. Gaussian, orthogonal signaling maximizes the ASE).

Similarly, Fig. 4 shows the ASE as a function of E_b/N_0, E_b being the received signal energy per information bit, for a set of selected cases. We remark again that the same values of T and F, optimized for vanishing small values of N_0, have been employed at each value of the SNR, while in the case of double signaling, the parameter β has been re-optimized for each value of the SNR. It is worth pointing out the large gain provided by the double signaling scheme proposed in Section V, even at low and medium SNRs.

Having previously shown the potential gains in terms of ASE provided by the proposed technique, we now analyze the performance of a practical coded scheme in terms of convergence threshold, by means of the powerful EXIT chart analysis [11], as well as in terms of BER. In both cases, we employed the rate-1/2 and rate-3/4 irregular LDPC codes [12] with codeword length 64800, proposed for the future 2nd generation Satellite Digital Video Broadcasting (DVB-S2) standard [19]. A QPSK modulation and a symmetric Gaussian pulse have been used in all cases. The single-signaling scenario described by (2) have been used, although we point out that all the results discussed below can be generalized to the double-signaling scheme (eq. (13)) as well.

First of all, a convergence threshold analysis, when the LDPC codes described above are used, has been carried out through EXIT chart analysis, as in [20]. In this scenario, the receiver can be seen as the serial concatenation of two component blocks, connected through an interleaver. The outer block is denoted as Check Node Decoder (CND), and its EXIT curve can be evaluated in closed form [20]. On the other hand, the inner block is the composition of the LDPC Variable Node Decoder (VND) and the employed equalization algorithm, namely, either the symbol-by-symbol or the proposed SIC algorithm with two self-iterations, and the relevant EXIT curves have been evaluated by means of numerical simulations. An automatic procedure has been developed, whose aim is to find the minimum E_b/N_0 for which the EXIT tunnel is open. In Fig. 5, the convergence thresholds of the considered LDPC codes are shown, parameterized by the spacings product FT, for both the symbol-by-symbol and the proposed SIC-based receiver. For comparison, we also show the capacity curve η_C and the maximal ASE, obtained by solving (12) for each value of E_b/N_0, in the considered scenario. Note that, for small enough values of the spectral efficiency (i.e., large values of the spacing FT), the interference is very small and the convergence thresholds correspond to those of the employed LDPC codes on the AWGN channel, namely about 0.5 dB (for the rate-1/2 code) and 3.8 dB (for the rate-3/4 code).

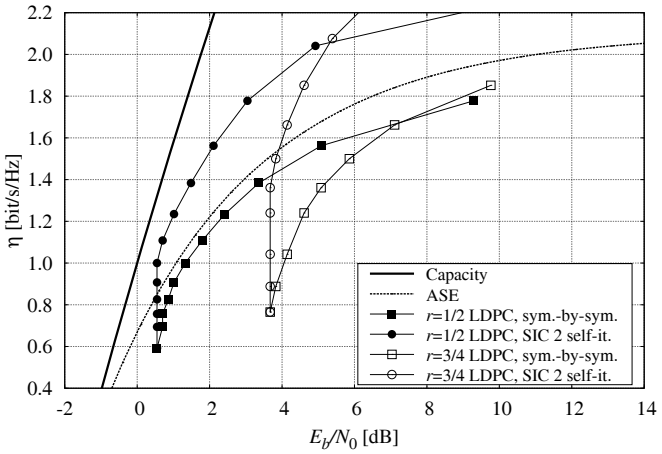

Fig. 5. Convergence thresholds for the two considered irregular LDPC codes, QPSK modulation and a Gaussian base pulse.

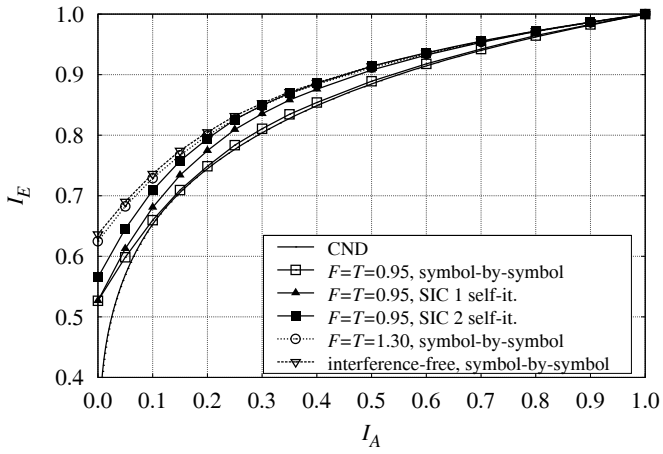

Fig. 6. EXIT chart for the rate-1/2 LDPC code, $E_b/N_0 = 1.9$ dB, QPSK modulation and a Gaussian base pulse.

Moreover, in this low-interference scenario the performance of the symbol-by-symbol receiver is almost the same as that of the more involved SIC algorithm. On the contrary, for large values of the spectral efficiency, corresponding to a large interference, the use of a SIC receiver allows an exceptional performance gain. By the way, the performance of the SIC receiver may even exceed the maximal ASE, since the latter has been evaluated assuming a symbol-by-symbol receiver.

Although not shown here due to the lack of space, the AIR corresponding to the maximal ASE curve shown in Fig. 5 intersects the value 1 bit/ch. use, which corresponds to the information rate of the rate-1/2 code (since it is mapped on a quaternary alphabet), at $E_b/N_0 = 1.5$ dB, from which an ASE of 1.11 bit/s/Hz and an optimal spacing $F = T = 0.95$ follow. At this value of the ASE, the performance of the considered rate-1/2 code is excellent, since the convergence threshold is about 1.9 dB when the symbol-by-symbol receiver is employed, thus the loss with respect to the maximal ASE is limited within a few tenths of dB.

We now discuss the EXIT chart, depicted in Fig. 6, corresponding to the rate-1/2 code and two values of the spacing, namely $F = T = 0.95$ as discussed above, and a highly suboptimal value $F = T = 1.3$, for which however an almost interference-free channel results. The relevant curves, corresponding to the two scenarios, have been obtained by means of numerical simulations working at $E_b/N_0 = 1.9$ dB, which is the convergence threshold when $F = T = 0.95$ and the symbol-by-symbol receiver is employed. From Fig. 6 some observations can be drawn: first, the use of the proposed SIC-based receiver, even with just one self-iteration, dramatically improves the EXIT curve in the strong-interference scenario. Moreover, by increasing the number of self-iterations from 1 to 2, a further improvement is possible. No improvement has been observed when performing further self-iterations. On the other hand, in the weak-interference scenario (i.e., FT large), the improvement stemming from the use of the SIC receiver is much more limited, since the symbol-by-symbol receiver almost performs as in the interference-free benchmark case.

In order to confirm the outcomes of the EXIT chart analysis discussed above, the BER performance is evaluated in the same scenario. At the receiver, the proposed SIC equalization

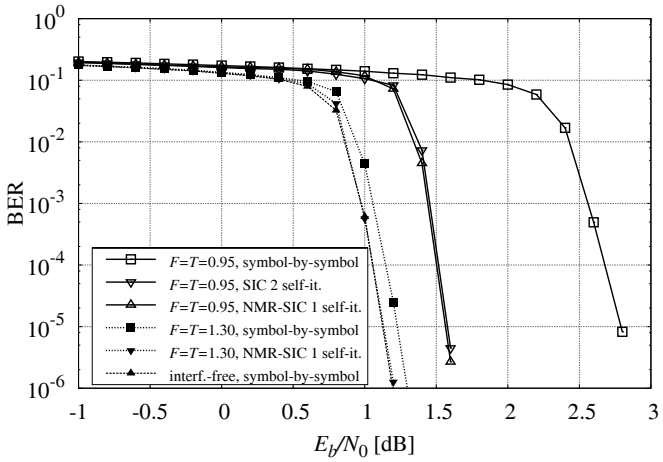

Fig. 7. BER performance of the considered LDPC-coded scheme, when a Gaussian pulse and a QPSK modulation are employed.

algorithms are iteratively activated along with the LDPC decoder, for an overall amount of 25 iterations. The process also stops if, by checking the code syndrome, a valid codeword is found before the 25^{th} iteration. Fig. 7 shows the BER as a function of E_b/N_0. Note that the convergence thresholds are in line with the results highlighted by the EXIT chart analysis of Fig. 5.[6] For example, the waterfall region for the strong-interference scenario and the symbol-by-symbol receiver begins at about 2.4 dB, whereas the convergence threshold was 1.9 dB. Similarly, both the considered SIC-based receivers outperform the symbol-by-symbol receiver of about 1 dB, that is exactly the same offset predicted in Fig. 5. We point out that, in all the BER simulations we carried out, the NMR-SIC with just one self-iteration always behaved as the SIC with two or more self-iterations, despite its lower complexity. Finally, we observe that, in the weak-interference scenario, the NMR-SIC receiver behaves exactly as the symbol-by-symbol receiver in the interference-free benchmark case.

[6]Since the EXIT chart analysis relies on a number of assumptions, namely infinite block length, infinite number of iterations, and Gaussian-distributed log-likelihood ratios, the waterfall region of practical systems is usually well beyond the threshold value predicted by the EXIT analysis.

VIII. Conclusions

We have proposed a way to improve the spectral efficiency of linear modulations with finite order constellations on an AWGN channel, achievable by a symbol-by-symbol receiver. This is obtained by reducing the spacing, in both time and frequency domains, between adjacent signals, hence introducing controlled interference, but at the same time making a better use of the available time and frequency resources. With respect to [8], which pursued a similar approach, a symbol-by-symbol detection algorithm is employed at the receiver, and the achievable spectral efficiency is used as a performance measure.

Moreover, we have shown that when two independent signals, that suitably span the time-frequency domain with a proper power allocation, are employed, along with a successive interference cancellation receiver, the performance gain is remarkable. The simulation results clearly pointed out that, when finite-order constellations (e.g., QPSK) are employed, orthogonal signaling can be largely suboptimal from the spectral efficiency point of view. On the contrary, when higher-order constellations are considered, the gain of the proposed schemes decreases. In summary, the proposed techniques can be seen as a low-complexity alternative to Gaussian shaping [4].

Finally, a low-complexity equalization scheme, based on the soft interference cancellation principle, has been proposed, and its performance in an LDPC-coded iteratively-decoded scheme evaluated in terms of EXIT chart and BER. The proposed receiver has a computational complexity only slightly larger than that of the symbol-by-symbol receiver, but allows excellent performance, even in strong-interference scenarios, when error-correcting codes designed for the AWGN channel are employed, without the need for a complete redesign of the coding scheme.

References

[1] W. Kozek and A. F. Molisch, "Nonorthogonal pulseshapes for multicarrier communications in doubly dispersive channels," *IEEE J. Select. Areas Commun.*, vol. 16, no. 8, pp. 1579-1589, Oct. 1998.

[2] T. Strohmer and S. Beaver, "Optimal OFDM design for time-frequency dispersive channels," *IEEE Trans. Commun.*, vol. 51, no. 7, pp. 1111-1122, July 2003.

[3] M. M. Hartmann, G. Matz, and D. Schafhuber, "Theory and design of multipulse multicarrier systems for wireless communications," in *Proc. Asilomar Conf. Signals, Systems, Comp.*, Nov. 2003, pp. 492-496.

[4] A. R. Calderbank and L. H. Ozarow, "Nonequiprobable signaling on the Gaussian channel," *IEEE Trans. Inform. Theory*, vol. 36, no. 4, pp. 726-740, July 1990.

[5] G. Colavolpe, A. Barbieri, and G. Caire, "Algorithms for iterative decoding in the presence of strong phase noise," *IEEE J. Select. Areas Commun.*, vol. 23, no. 9, pp. 1748-1757, Sept. 2005.

[6] F. Rusek and J. B. Anderson, "On information rates of faster than Nyquist signaling," in *Proc. IEEE Global Telecommun. Conf.*, San Francisco, CA, USA, Nov. 2006.

[7] ——, "Maximal capacity partial response signaling," in *Proc. IEEE Intern. Conf. Commun.*, June 2007, pp. 821-826.

[8] ——, "The two dimensional Mazo limit," in *Proc. IEEE International Symp. Inform. Theory*, Sept. 2005, pp. 970-974.

[9] X. Wang and H. V. Poor, "Iterative (turbo) soft interference cancellation and decoding for coded CDMA," *IEEE Trans. Commun.*, vol. 47, pp. 1046-1061, July 1999.

[10] J. Boutros and G. Caire, "Iterative multiuser joint decoding: unified framework and asymptotic analysis," *IEEE Trans. Inform. Theory*, vol. 48, no. 7, pp. 1772-1793, July 2002.

[11] S. ten Brink, "Convergence behavior of iteratively decoded parallel concatenated codes," *IEEE Trans. Commun.*, vol. 49, no. 10, pp. 1727-1737, Oct. 2001.

[12] T. Richardson and R. Urbanke, "The capacity of low density parity check codes under message passing decoding," *IEEE Trans. Inform. Theory*, vol. 47, pp. 599-618, Feb. 2001.

[13] D. Gabor, "Theory of communication," *J. IEE, London*, vol. 93, no. 26, pp. 429-457, Nov. 1946.

[14] A. Barbieri, G. Caire, and U. Mitra, "An approximate eigenmode decomposition for doubly-selective wireless channels," in *Proc. ICASSP*, Las Vegas, NV, Mar.-Apr. 2008.

[15] K. Yao, "Error probability of asynchronous spread spectrum multiple access communication systems," *IEEE Trans. Commun.*, vol. 25, no. 8, pp. 803-809, Aug. 1977.

[16] N. Merhav, G. Kaplan, A. Lapidoth, and S. S. Shitz, "On information rates for mismatched decoders," *IEEE Trans. Inform. Theory*, vol. 40, no. 6, pp. 1953-1967, Nov. 1994.

[17] D. M. Arnold, H.-A. Loeliger, P. O. Vontobel, A. Kavčič, and W. Zeng, "Simulation-based computation of information rates for channels with memory," *IEEE Trans. Inform. Theory*, vol. 52, no. 8, pp. 3498-3508, Aug. 2006.

[18] C. Douillard, M. Jezequel, C. Berrou, A. Picart, P. Didier, and A. Glavieux, "Iterative correction of intersymbol interference: turbo-equalization," *European Trans. Telecommun.*, vol. 6, no. 5, pp. 507-511, Sept./Oct. 1995.

[19] ETSI, "ETSI - DVBS2 74r13, Digital Video Broadcasting (DVB): Second generation framing structure, channel coding and modulation systems for Braoadcasting, Interactive Services, News Gathering and other broadband satellite applications," 2003.

[20] S. ten Brink, G. Kramer, and A. Ashikhmin, "Design of low-density parity-check codes for modulation and detection," *IEEE Trans. Commun.*, vol. 52, pp. 670-678, Apr. 2004.

Alan Barbieri received the Dr.Ing. degree in Telecommunications Engineering (cum laude) and the Ph.D. degree in Information Technology from the University of Parma, Parma, Italy, in 2003 and 2007, respectively.

Since November 2008 he is an associate professor at the Scuola Superiore Sant'Anna, Pisa, Italy. Previously, he held a post-doc position at the Dept. of Information Technology, University of Parma. In 2007 he was a visiting scholar at the Ming Hsieh Department of Electrical Engineering, University of Southern California, Los Angeles, CA. During summer 2008 he was a visiting faculty at the Qualcomm Corporate R&D Center, Qualcomm Inc., San Diego, CA.

His main research interests include digital transmission theory and information theory, with particular emphasis on channel coding, iterative joint detection and decoding algorithms, estimation of unknown parameters and algorithms for synchronization. He participates in several research projects funded by the European Space Agency (ESA-ESTEC) and important telecommunications companies.

Dario Fertonani (S'06) was born in Mantua, Italy, in 1980. He received the Dr.Ing. degree (cum laude) in telecommunications engineering in 2004 and the Ph.D degree in Information Technology in 2008, both from the University of Parma, Italy. Currently, he holds a post-doc position at the Scuola Superiore Sant'Anna, Pisa, Italy, and he is also a visiting scholar at the Arizona State University, Tempe, AZ.

His research interests include various topics in digital communications and information theory, with particular interest on design issues related to iterative detection/decoding over channels with memory and channels with impulse noise.

Giulio Colavolpe received the Dr. Ing. degree in Telecommunications Engineering (cum laude) from the University of Pisa, Italy, in 1994 and the Ph.D. degree in Information Technology from the University of Parma, Italy, in 1998. Since 1997, he has been at the University of Parma, Italy, where he is now an Associate Professor of Telecommunications. In 2000, he was Visiting Scientist at the Institut Eurécom, Valbonne, France.

His main research interests include digital transmission theory, adaptive signal processing, channel coding and information theory. He is also co-author of the book *Detection Algorithms for Wireless Communications, with Applications to Wired and Storage Systems* (New York: John Wiley & Sons, 2004). He received the best paper award at the 13th International Conference on Software, Telecommunications and Computer Networks (SoftCOM'05) and at the IEEE International Conference on Communcations (ICC 2008).